ELSEVIER

International Journal of Heat and Fluid Flow 19 (1998) 522–532

International Journal of
HEAT AND
FLUID FLOW

High-Schmidt number mass transfer through turbulent gas–liquid interfaces

Isabelle Calmet [a], Jacques Magnaudet [b,*]

[a] *Laboratoire de Mécanique des Fluides, UMR CNRS 6598, Ecole Centrale de Nantes, 1 rue de la Noe, B.P. 92101, 44321 Nantes, Cedex 3, France*
[b] *Institut de Mécanique des Fluides de Toulouse, UMR CNRS 5502, 2 avenue Camille Soula, 31400 Toulouse, France*

Abstract

This paper reports some new results concerning the structure of the concentration field and the mechanisms of mass transfer at flat, turbulent, gas–liquid interfaces, especially in the limit of high-Schmidt numbers. The problem is investigated using the Large Eddy Simulation technique applied to two different kinds of interfaces, namely a sheared-driven interface and a shear-free surface. Statistical results show that the concentration field is greatly affected by the structure of the turbulence in the diffusive sublayer located just below the interface. When no shear is applied on the interface, the instantaneous picture of the interfacial structures reveals that the concentration field is organized in large patches that mirror the upwelling structures coming from the core of the flow. In contrast at a sheared interface the concentration field is organized in elongated structures of much smaller spanwise extent. The shape of these structures is found to result from the combined effect of advection by the streamwise velocities which are themselves organized in streaks, and of the vertical motions induced by bursting events. For both kinds of interfaces, it is found that the concentration fluctuations are closely related to the horizontal turbulent motions that stretch the interface. The results of the simulations are used to check several mass transfer models. In accordance with instantaneous visualizations and statistical properties of the concentration field, the model of McCready et al. (AIChE J.32 (1986) 1108–1115) involving the surface divergence appears to be the most suitable for predicting the mass transfer coefficient through gas–liquid interfaces.

Keywords: Turbulence; Mass transfer; Large-eddy simulation; Gas-liquid interface; Coherent structure

1. Introduction

Diffusion at high-Schmidt numbers through turbulent gas–liquid interfaces occurs in many geophysical or industrial processes. It is for example the basic situation encountered in the exchange of slightly soluble gases like O_2 or CO_2 between the atmosphere and the oceans or the lakes. For such gases the diffusive sublayer in the liquid is so thin that the transfer is entirely governed by the structure of the turbulent field in the immediate vicinity of the interface. To understand such gas transfer processes, it is obviously highly desirable to perform simultaneous analyses of concentration and velocity fluctuations in the interfacial region in terms of both statistics and turbulent structures. Unfortunately this goal is very difficult to achieve experimentally: instantaneous measurement of concentration by means of microprobes is still under development and parasitic phenomena like interface contamination by impurities or capillary ripples occur very frequently in these experiments. Direct Numerical Simulation would be a perfect tool for that purpose but is very limited in practice since the number of grid points required to capture the smallest scalar scales grows with the Reynolds (Re) and Schmidt (Sc) numbers like $Sc^3Re^{9/4}$. Nevertheless, the same kind of information can be obtained by using the Large Eddy Simulation (LES) technique which avoids this limitation, provided the small scales do not prevail in the transfer process and their major effects on the large scales are correctly modelled. Recently this approach has been proved to provide very good results in the study of mass transfer at a solid wall: Calmet (1995) and Calmet and Magnaudet (1997) showed that the LES approach using recent advances made in the formulation of subgrid-scale models gives mass transfer rates and characteristics of the mean and fluctuating concentration fields in very good agreement with the most advanced experimental studies.

The present paper reports some results obtained using the same technique for studying diffusion through flat gas–liquid interfaces at two very different Schmidt numbers ($Sc = \nu/D_\mu$, ν and D_μ denoting the kinematic viscosity and the molecular diffusivity, respectively), namely $Sc = 1$ and $Sc = 200$. Two kinds of interfaces are considered by computing two different high-Re turbulent flows: a liquid layer driven by the interfacial shear is used to study mass transfer at a sheared interface while an open channel flow is employed for investigating mass transfer at a shear-free surface (Fig. 1). In both cases tangential velocity fluctuations can subsist up to the surface in contrast with the situation encountered at a solid wall. However the turbulence characteristics observed below the two interfaces are

* Corresponding author.

0142-727X/98/$ – see front matter
PII: S0142-727X(98)10017-6

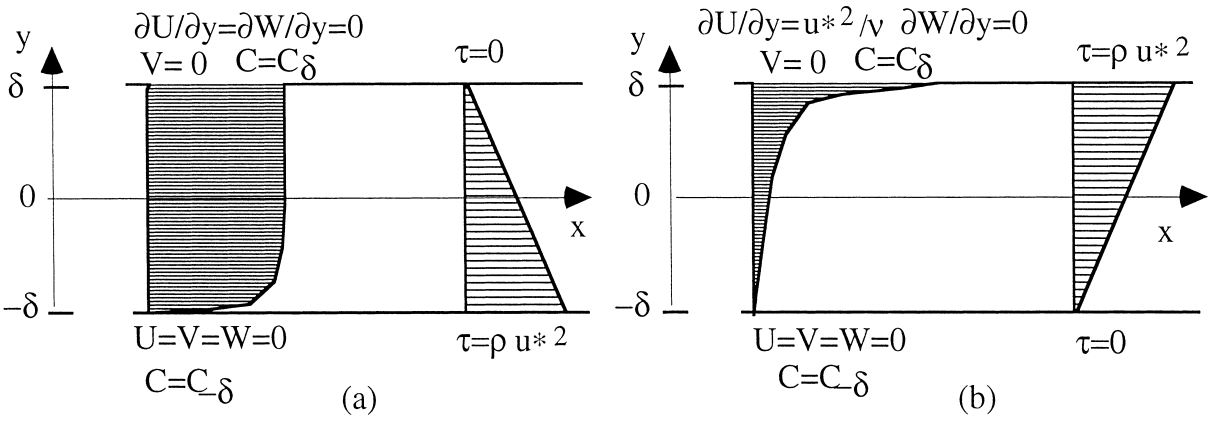

Fig. 1. Sketch of the flow configurations. (a) Shear-free surface; (b) Sheared interface.

dramatically different: when a non-zero shear acts directly on the interface, turbulence is produced right there, whereas in the open channel configuration turbulence is created at the bottom wall and is then self-transported towards the free surface. After a brief description of the LES approach (Section 2), some statistical results are presented in Section 3 together with systematic comparisons showing the effect of the shear or of the Schmidt number on the concentration field. In Section 4 attention is focused on the relationship between instantaneous mass flux at high Schmidt number and turbulent structures present below the interfaces. Finally, results of the simulations are used to check several mass transfer models in Section 6.

2. Description of the computations

The flow fields corresponding to the two situations described above are computed using the LES code already developed at IMFT (Calmet, 1995). Basically this code solves the three-dimensional governing equations filtered in space by the computational grid, namely

$$\frac{\partial \bar{V}_i}{\partial x_i} = 0, \tag{1a}$$

$$\frac{\partial \bar{V}_i}{\partial t} + \frac{\partial}{\partial x_j}(\bar{V}_i \bar{V}_j) = -\frac{\partial \bar{P}_i}{\partial x_i} + \frac{\partial}{\partial x_j}[2\nu \bar{S}_{ij} - \tau_{ij}], \tag{1b}$$

$$\frac{\partial \bar{C}}{\partial t} + \frac{\partial}{\partial x_j}(\bar{C}\bar{V}_j) = \frac{\partial}{\partial x_j}\left[D_\mu \frac{\partial \bar{C}}{\partial x_j} - q_j\right], \tag{1c}$$

where $\bar{S}_{ij} = \frac{1}{2}(\partial \bar{V}_i/\partial x_j + \bar{\partial} V_j/\partial x_i)$ denotes the resolved strain rate tensor. The effect of the unresolved subgrid scales appears in Eqs. (1b) and (1c) through the subgrid stress $\tau_{ij} = \overline{V_i V_j} - \bar{V}_i \bar{V}_j$ and the subgrid flux $q_j = \overline{CV_j} - \bar{C}\bar{V}_j$. These subgrid scale terms are closed using the Dynamic Mixed Model (DMM) developed by Zang et al. (1993) and extended to the subgrid scalar flux by Calmet and Magnaudet (1997). In this model the anisotropic part of τ_{ij} is written under the form

$$\tau_{ij} - \tfrac{1}{3}\tau_{kk}\delta_{ij} = L_{ij} - \tfrac{1}{3}L_{kk}\delta_{ij} - 2\nu_T \bar{S}_{ij} \tag{2a}$$

with $L_{ij} = \overline{\bar{V}_i \bar{V}_j} - \overline{\bar{V}_i}\,\overline{\bar{V}_j}$. Similarly the scalar flux is written under the form

$$q_j = -D_T \frac{\partial \bar{C}}{\partial x_j} + Lc_j \tag{2b}$$

with $Lc_j = \overline{\bar{C}\bar{V}_j} - \overline{\bar{C}}\,\overline{\bar{V}_j}$. The important feature of the DMM is that the Leonard terms L_{ij} and L_{cj} which are by far the most important subgrid-scale contribution in that formulation (see Calmet, 1995) are computed explicitly by re-filtering the resolved fields $\bar{V}_i$ and $\bar{C}$ and their products on the computational grid. Consequently the subgrid-scale stress (resp. flux) is not forced to align with the resolved rate-of-strain (resp. concentration gradient). Following Smagorinsky, the subgrid viscosity and diffusivity are connected to the local grid scale $\bar{\Delta} = (\bar{\Delta}_1 \bar{\Delta}_2 \bar{\Delta}_3)^{1/3}$ and to the local strain rate $|\bar{S}| = (2\bar{S}_{ij}\bar{S}_{ij})^{1/2}$ through the well-known expressions:

$$\nu_T = C\bar{\Delta}^2|\bar{S}| \quad \text{and} \quad D_T = C_c\bar{\Delta}^2|\bar{S}| \tag{3}$$

where C and C_c are the dimensionless coefficients to be determined dynamically. The computation of C and C_c is carried out using the Germano (1992) identity and the double-filtering procedure first proposed by Germano et al. (1991). A thorough description of this dynamic computation is given in Calmet and Magnaudet (1997) to which the reader is referred. The result of this procedure is to produce subgrid scale coefficients which vary in both time and space. It is worth noting that no averaging procedure in planes of homogeneity is used here, so that the values of C and C_c employed in the computations are actually closely related to the local and instantaneous features of the turbulent field.

The flows are studied at a single Reynolds number $\mathrm{Re}^* = 1280$, based on the total depth 2δ and the friction velocity u^* (at the bottom wall or at the interface, respectively). The computational box of size $2\pi\delta \times 2\delta \times 3\pi\delta/4$ is discretized with a $32 \times 64 \times 64$ grid for $\mathrm{Sc} = 1$ and with a $32 \times 86 \times 64$ grid for $\mathrm{Sc} = 200$. This grid is uniform in the streamwise x and spanwise z directions and highly stretched in the normal direction in order to resolve properly the diffusive sublayer up to $y^+ \approx 0.01$ in the sheared case for $\mathrm{Sc} = 200$. The grid spacing and the size of the computational box were chosen by reference to a previous channel flow LES study (Calmet and Magnaudet, 1997) in which it was found that they led to numerical results in very good agreement with experiments for both dynamical and scalar properties. The boundary conditions are specified in Fig. 1. They assume periodicity of all variables (except the mean pressure) in the streamwise and spanwise directions. No-slip conditions are imposed at the bottom wall. In contrast the conditions imposed on both interfaces (upper plane) state that the normal velocity as well as the fluctuating shear stresses are zero, allowing the tangential velocity fluctuations u' and w' to subsist up to the surface. Assuming an immediate renewal of the concentration at the upper and lower boundaries, two different constant values (C_δ and $C_{-\delta}$) are imposed there and drive the mass transfer process. After the numerical solution

has reached a statistically steady state, time integration is carried out over several turnover times in order to perform statistical averages (denoted by $\langle\ \rangle$) in time as well as in (x,z) planes.

3. Statistics of the concentration field

To discuss the statistical behavior of the various quantities of interest we introduce the friction velocity u^* defined as the square root of the shear stress at the interface (resp. at the bottom wall) in the sheared case (resp. in the shear-free case) and the reference concentration c^* defined by $c^* = (D_u/u^*)(\partial\langle\bar{C}\rangle/\partial y)_{y=\delta}$. It is important to notice that the friction velocity u^* can be used as a normalizing factor even in the shear-free case because it is found in this situation that, whatever the distance between the bottom wall and the interface, the non-dimensional turbulent kinetic energy K/u^{*2} reaches values of order unity at the interface. Using u^* one can also define a normalized interfacial distance $y^+ = (\delta - y)u^*/\nu$ which originates at the interface. In the immediate vicinity of the interface it can be shown (Calmet, 1995) that the normalized velocity fluctuations obey $u' = a_0 + a_2 y^{+2} + \cdots$, $v' = b_1 y^+ + b_3 y^{+3} + \cdots$ and $w' = c_0 + c_2 y^{+2} + \cdots$ while the normalized concentration fluctuation obeys $c' = d_1 y^+ + d_3 y^{+3} + \cdots$ Using these expansions one can demonstrate that the normalized diffusive sublayer thickness $\delta_c^+ = \delta_c u^*/\nu$ is related to the viscous sublayer thickness δ_u^+ through

$$\delta_c^+ \propto \sqrt{\delta_u^+}\,\mathrm{Sc}^{-1/2}. \tag{4}$$

In Fig. 2 the mean concentration $C^+ = (C_\delta - \langle\bar{C}\rangle)/c^*$ is plotted vs. the normalized interfacial distance y^+. Since the diffusive sublayer is the region where the concentration profile C^+ typically evolves like Sc y^+, δ_c^+ can be directly estimated graphically. One finds $\delta_c^+ \approx 1.9$ at $\mathrm{Sc} = 1$ and $\delta_c^+ \approx 0.12$ at $\mathrm{Sc} = 200$ near the sheared interface. Close to the shear-free surface the same technique yields $\delta_c^+ \approx 5$ at $\mathrm{Sc} = 1$ and $\delta_c^+ \approx 0.35$ at $\mathrm{Sc} = 200$. Below the sheared interface, the simulation indicates $\delta_c^+ \approx 3$ in accordance with the measurements of McLeish and Putland (1975). This value is smaller than the one found near a rigid wall because close to an interface viscous effects only affect the slope of the velocity fluctuations but have little effect on their magnitude. Injecting the latter value in the theoretical law (4) yields $\delta_c^+ \approx 1.73$ at $\mathrm{Sc} = 1$ and $\delta_c^+ \approx 0.12$ at $\mathrm{Sc} = 200$, in good agreement with the graphical estimates. For a shear-free surface, the value of δ_u^+ cannot be determined through the velocity profile. However once δ_c^+ is known, δ_u^+ can be estimated through (4). Using the results corresponding to both Schmidt numbers one finds $\delta_u^+ \approx 25$. This very large value occurs because close to the shear-free surface small-scale structures are quite rare, owing to the absence of shear. As conjectured by Hunt (1984) this feature yields a large value of the Kolmogorov microscale and thus large values of δ_u^+.

Fig. 3 represents the r.m.s. values of the concentration c' normalized by the difference of concentration ΔC between the interface and the bulk. These values reach a well-defined maximum in the buffer region of C^+, i.e. between the diffusive sublayer where $C^+ = \mathrm{Sc}\ y^+$ and the log-layer where $C^+ \propto \mathrm{Log}(y^+)$. Owing to the $\mathrm{Sc}^{-1/2}$ dependency of the diffusive sublayer thickness, this maximum is reached much closer to the

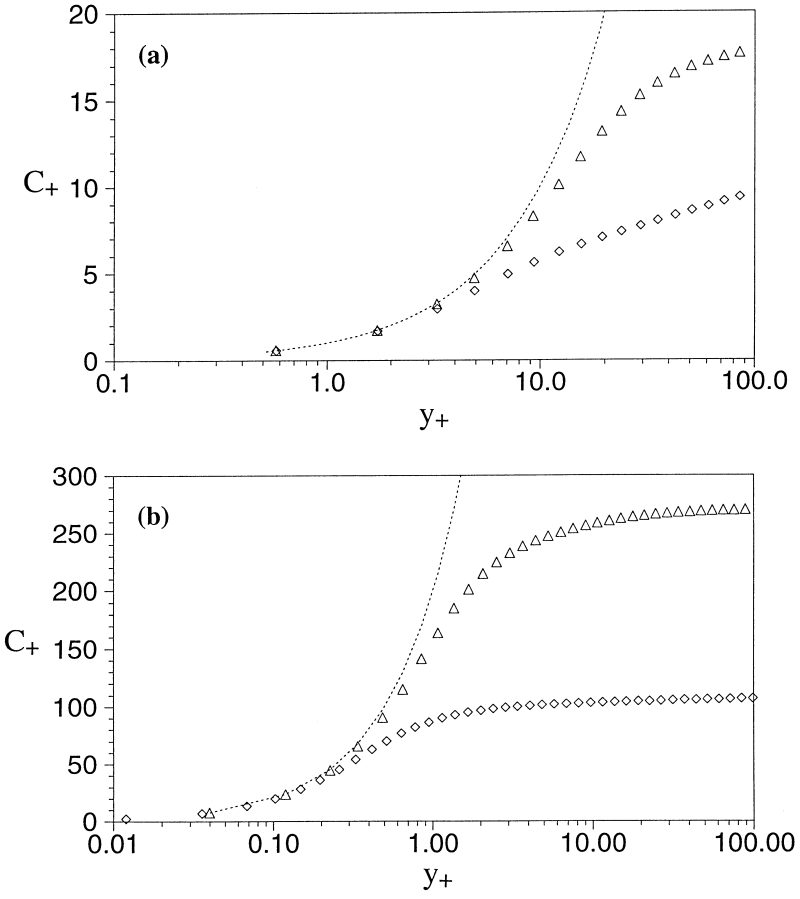

Fig. 2. Mean concentration profiles at (a) $\mathrm{Sc} = 1$, (b) $\mathrm{Sc} = 200$: $\triangle$ Shear-free surface; $\diamond$ Sheared interface; $C^+ = \mathrm{Sc}\ y^+$.

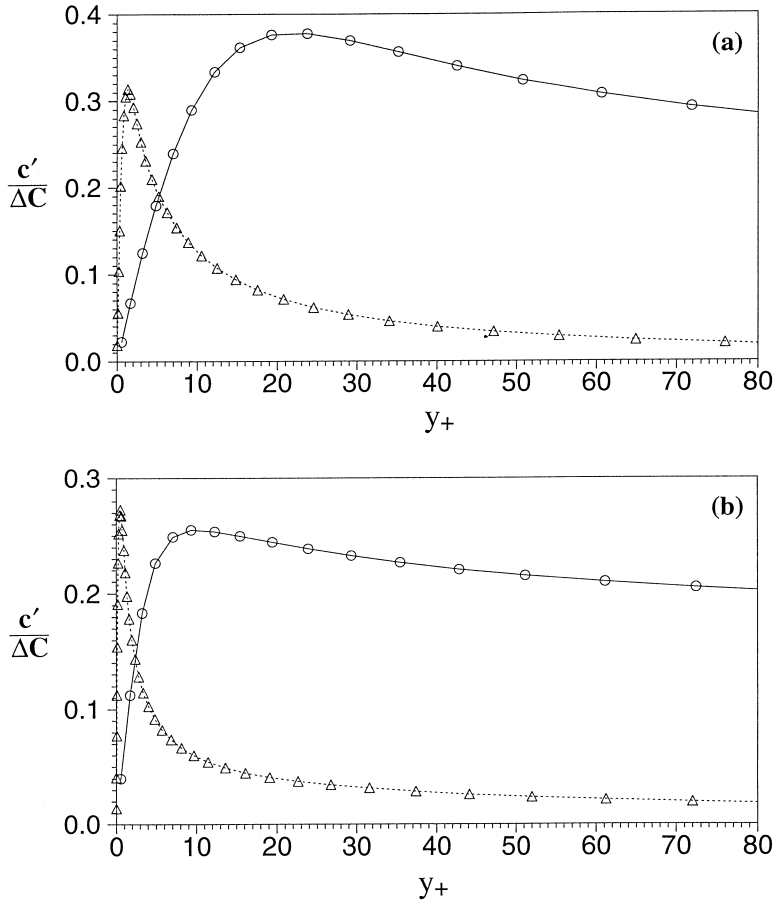

Fig. 3. Fluctuations of concentration close to (a) the shear-free surface, (b) the sheared interface: o-o Sc = 1; △..△ Sc = 200.

interface at Sc = 200 than at Sc = 1. Below the sheared interface the maximum value of c' is about 0.25 for both Schmidt numbers. Turbulence characteristics in the buffer region of concentration greatly influences the fluctuations c'. Indeed, in the sheared case, the velocity fluctuations reaching their maximum right at the interface, the maximum of c' at Sc = 200 is somewhat higher than at Sc = 1 (0.28 instead of 0.25). In contrast, near the shear-free surface the turbulence intensity decreases slightly when the interface is approached. Consequently an opposite behavior of c' is found, i.e. the maximum of c' is found to be 0.38 at Sc = 1 whereas it decreases to 0.31 at Sc = 200. Moving away from the interface, c' becomes nearly zero at Sc = 200 since the mean concentration is essentially constant over most of the flow. In contrast for Sc = 1, a mean concentration gradient persists throughout the bulk because the mass flux crossing the flow from $y = \delta$ to $y = -\delta$ is much larger than in the high-Sc case. As can be seen in Fig. 3, this gradient induces significant r.m.s. intensities far from the interface. Although turbulence is weaker near the shear-free surface than near the sheared interface, c' is more intense in the first case owing to the presence of much larger, nearly non-dissipative eddies. This trend is confirmed by the budget of $\langle c'^2 \rangle$ whose various contributions (already defined by Calmet and Magnaudet, 1997) are displayed in Fig. 4 for Sc = 1. At the location where c' reaches its maximum value (i.e. $y_+ \approx 10$ below the sheared interface and $y_+ \approx 25$ below the shear-free surface), the ratio between the production term and the dissipation rate is found to reach a significantly higher value below the shear-free interface ($P_c/\varepsilon_c \approx 3.9$) than below the sheared interface ($P_c/\varepsilon_c \approx 2.0$). In this budget, a cascade term coming from the explicit computation of the Leonard terms in the LES equations also appears. In agreement with previous conclusions, it is seen that this contribution is negligible below the shear-free surface because of the lack of small-scale structures, while it represents about 30% of the turbulent transport below the sheared interface.

Another interesting information is provided by the skewness factors $S(c')$ and $S(v')$ shown in Fig. 5. These skewness factors indicate that the largest events affecting the concentration field are directly related to the largest events affecting the normal velocity fluctuation v'. As will be seen below, the events responsible for the asymmetry of the concentration field are either turbulent structures ejected from the bottom wall and reaching the shear-free interface, or sweeping events following the ejection process below the sheared interface. So, in both cases $S(c')$ is negative close to the interface since the upwelling velocities responsible for $S(v') > 0$ always carry concentrations which are smaller than the average concentration.

4. Relationship between the turbulent structures and the concentration field

Figs. 6 and 8 represent the instantaneous iso-contours of the vertical velocity v' and of the concentration c' at Sc = 200 in horizontal planes located in the diffusive sublayer, i.e. very close to each interface. Positive values are plotted with solid lines while dotted lines represent negative values. A direct comparison of the iso-contours of v' and c' reveals that the dynamics of the concentration field is highly correlated with the

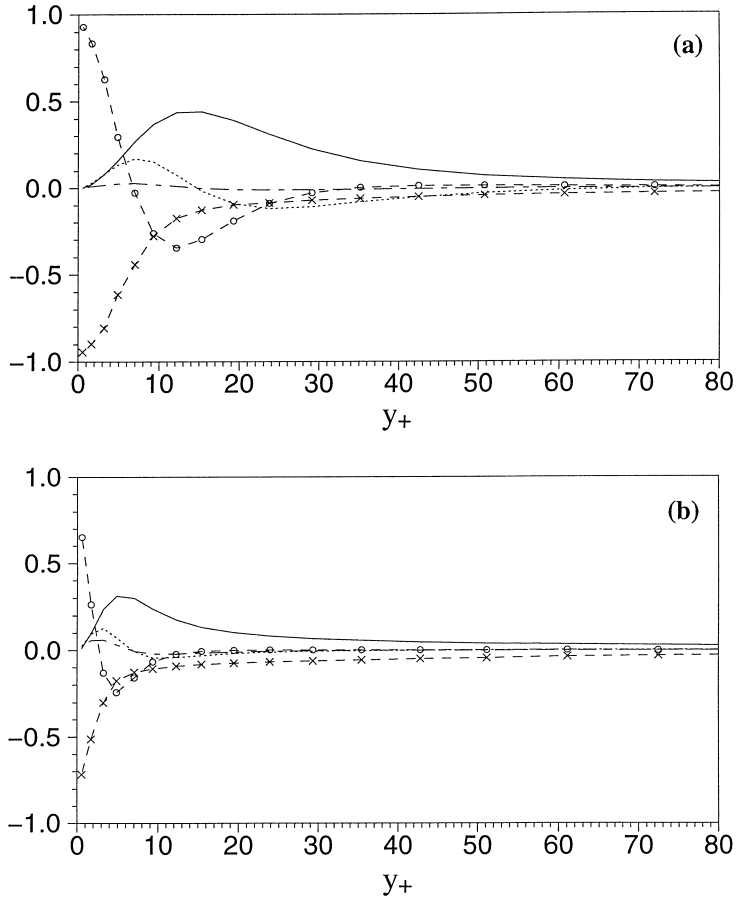

Fig. 4. Budget of $\langle c'^2 \rangle$ for Sc = 1 close to (a) the shear-free interface, (b) the sheared interface. —— production P_c; - - - turbulent transport T_c; – – – cascade term TL_c; ○ – – ○ molecular diffusion D_c; × – – × pseudo-dissipation ε_c. All terms are normalized by $D_\mu/c^{*2}u^{*2}$.

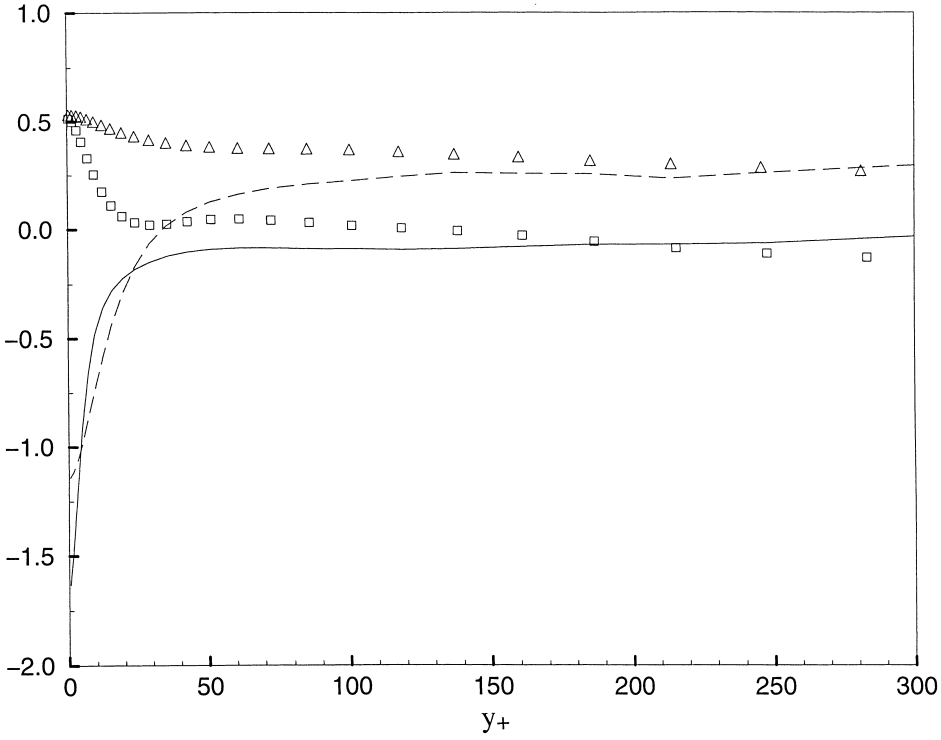

Fig. 5. Skewness factors close to the shear-free surface: △ $S(v')$; - - - $S(c')$ (Sc = 1) and close to the sheared interface: □ $S(v')$; —— $S(c')$ (Sc = 1).

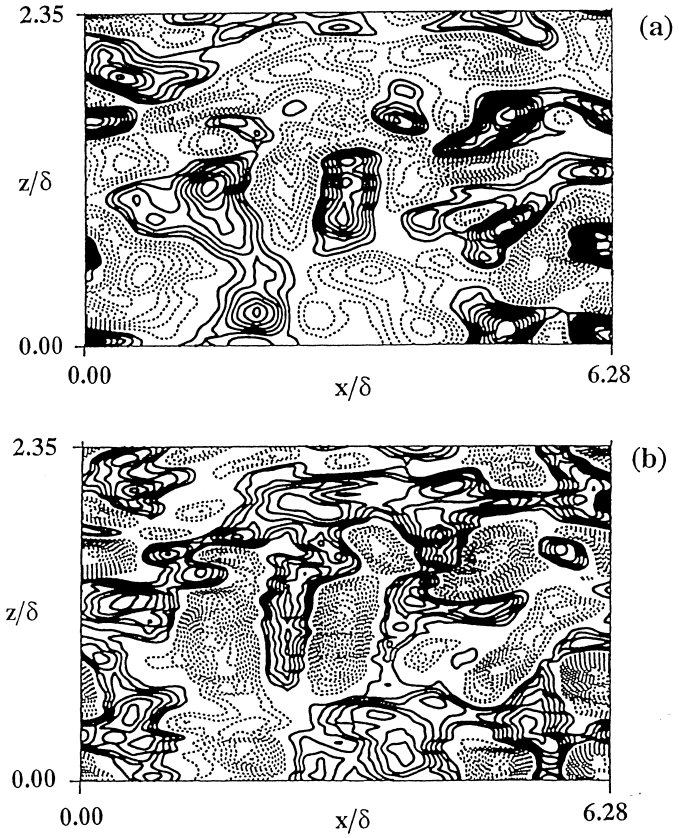

Fig. 6. Instantaneous iso-values of (a) v' and (b) c' close to the shear-free interface ($y_+ \approx 0.1$).

large-scale structures present near each interface. The large patches that reach the shear-free surface ($v' > 0$) or go away from it ($v' < 0$) carry low ($c' < 0$) and high ($c' > 0$) concentration, respectively. In this case, the dynamics is simple enough to observe a mirror-image between the iso-contours of v' and those of the concentration fluctuations. This means that the driving mechanism of the mass transfer is the renewal of the surface by the structures coming from the bottom wall. It is particularly interesting to observe the horizontal motions on the interface itself. For that purpose the instantaneous streamlines corresponding to Fig. 6 are plotted in Fig. 7. The relation between the horizontal interfacial motions and the turbulent events can be quantified by introducing the so-called surface divergence defined by

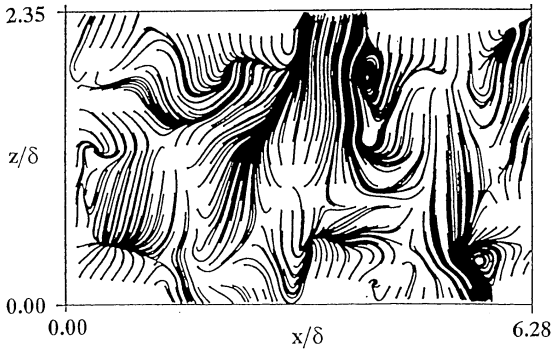

Fig. 7. Instantaneous streamlines on the shear-free interface.

$$\nabla_s \cdot \mathbf{v}_s = \beta(x,z,t) = \{\partial u'/\partial x + \partial w'/\partial z\}_s = -\{\partial v'/\partial y\}_s. \quad (5)$$

The interfacial sources defined by $\beta > 0$ (resp. the sinks defined by $\beta < 0$) corresponding to upwelling (resp. downwelling) motions are easily seen in Fig. 7. Coming back to the iso-contours of c', it appears that the concentration fluctuations are very closely related to the compression and dilation of the interface.

Near the sheared interface, the normal velocity fluctuations induced by the interfacial bursts have a very different structure: iso-contours of v' (Fig. 8(a)) show that these events have a small lateral extent and are elongated in the streamwise direction. The same is true for c' but the concentration field (Fig. 8(b)) seems to be less organized than the vertical velocity field and the relation between the two pictures is less simple than in the shear-free case. In contrast iso-contours of the streamwise velocity fluctuations (Fig. 9) reveal that u' is clearly organized in regular streaks very similar to those present in usual boundary layers. A cross-section (y,z) of the c'-field is displayed on Fig. 10 for $Sc = 1$ and $Sc = 200$. These pictures have to be compared with their counterpart in wall turbulence described by Calmet and Magnaudet (1997). From this comparison, it becomes obvious that in the present case the concentration field is organized in a spanwise succession of positive and negative fluctuations, exactly like near a solid wall. In spite of the disorder present in Fig. 8(b), this would suggest that close to a sheared interface the concentration field is also organized in streaky structures. On the other hand, there is no doubt that the vertical motions reaching the interface (which result from the cycle of life of the streaks) are the source of the concentration fluctuations like in the shear-free case. Thus the complete scenario appears to be that, once

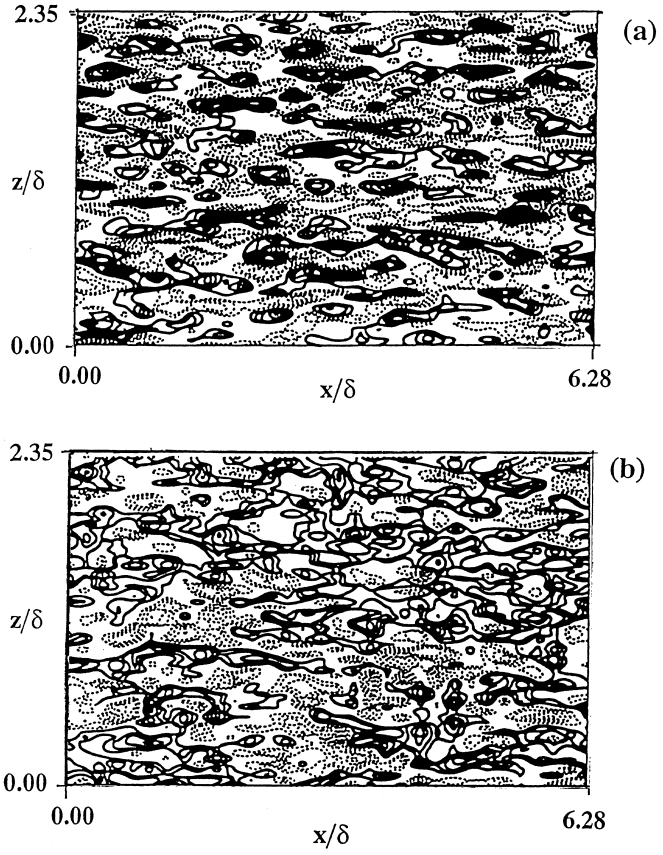

Fig. 8. Instantaneous iso-values of (a) v' and (b) c' close to the sheared interface ($y_+ \approx 0.1$).

the concentration fluctuations have been created by v' in the diffusive sublayer, they are transported and stretched by the large scales of the turbulent field and especially by the longitudinal streaks. Thus the structure of the concentration field is a mixture between the structure of v' in the viscous sublayer and the streaky structure of u', giving a more complicated picture than near a solid wall or near the shear-free surface.

5. Comparison with some mass transfer models

Deriving simple predictive mass transfer models has been a subject of great importance in chemical engineering for a long time. Generally mass transfer efficiency is measured by defining a mass transfer velocity, K_L, directly proportional to the mass flux entering the liquid. Most of the mass transfer models state that the transfer is controlled by the molecular diffusivity D_μ and by a so-called renewal time τ. From dimensional evidence one then obtains (Danckwerts, 1951)

$$K_L = (D_\mu/\tau)^{1/2}. \tag{6}$$

The key problem in such models lies obviously in the prediction of τ. One can distinguish between models based on a *global* property of turbulence, such as the turbulent Reynolds number Re_T defined with the aid of the integral scale L_∞ and some velocity scale u' ($Re_T = 2L_\infty u'/v$), and models based on a local property able to characterize the turbulence on the interface itself.

The oldest and simplest models are of course those based on a global property of the turbulence. Depending on the range of scales which is assumed to govern the transfer, two kinds of models have emerged. If one assumes that the large scales dominate the transfer, one obtains $\tau \propto L_\infty/u'$. This yields (Fortescue and Pearson, 1967)

$$K_L/u' = C_{LS} Sc^{-1/2} Re_T^{-1/2}, \tag{7}$$

where the constant C_{LS} is generally set to 1.07. In contrast if one assumes that the transfer is governed by the small scales, the relevant time scale becomes $\tau \propto (v/\varepsilon)^{1/2}$ where ε denotes the dissipation rate. Then one obtains (Banerjee et al., 1968; Lamont and Scott, 1970)

$$K_L/u' = C_{SS} Sc^{-1/2} Re_T^{-1/4}, \tag{8}$$

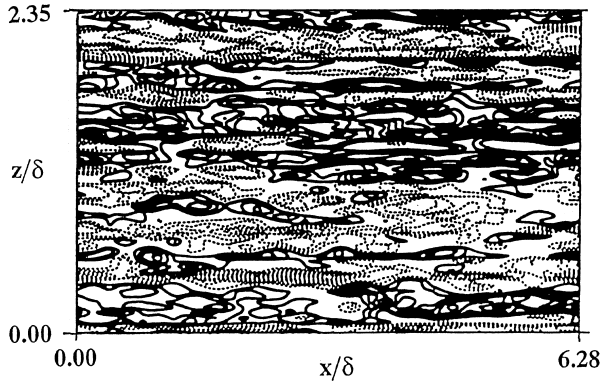

Fig. 9. Instantaneous iso-values of u' below the sheared interface ($y_+ \approx 1.7$).

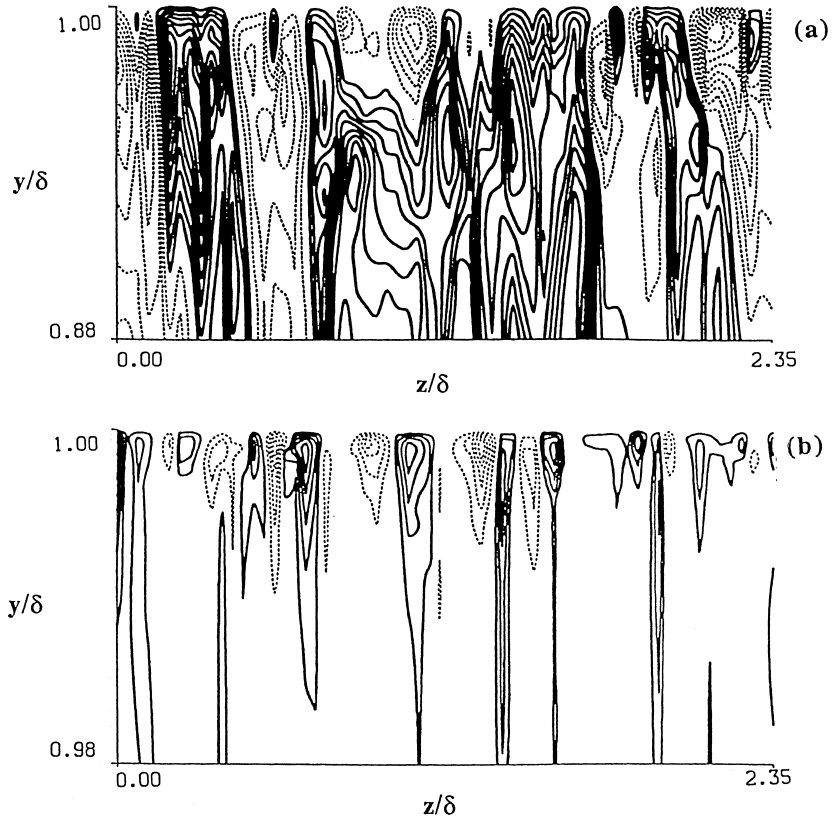

Fig. 10. Instantaneous iso-values of c' in a plane (y,z) below the sheared interface (a) $Sc = 1$, (b) $Sc = 200$.

where the constant C_{SS} is generally set to 0.25. Therefore the two models differ essentially by the exponent of the turbulent Reynolds number.

More recently, several models based on a local property of the turbulence evaluated right at the interface have appeared. The simplest one was proposed by Banerjee (1990). This author simply assumes that the turbulent events that control mass transfer are the large-scale bursts coming either from the interfacial region (when turbulence is produced directly at the interface) or from the bottom of the flow (when no shear acts on the free surface). Thus, denoting by f_B the bursting frequency and assuming that $\tau \propto f_B^{-1}$, the mass transfer coefficient is given by

$$K_L/u^* = (f_B^{-1}u^{*2}/v)^{-1/2}Sc^{-1/2}. \quad (9)$$

McCready et al. (1986) derived a more sophisticated model taking into account the complete range of turbulent scales by solving the instantaneous concentration equation in the diffusive sublayer at a sheared interface. For that purpose they injected in this equation a normal velocity signal recorded experimentally. This signal evolved linearly with according to the law $v' = \beta(t)(\delta - y)$. In this approach the characteristic time is obviously $\tau \propto \langle\beta^2\rangle^{-1/2}$. The results obtained by McCready et al. showed that the mass transfer coefficient follows the law

$$K_L/u^* = 0.71\langle\beta^2\rangle^{1/4}Sc^{-1/2}. \quad (10)$$

Having recalled the form and the assumptions associated to these models, it is of particular interest to compare the values of the mass transfer coefficient K_L/u^* predicted by these models with those obtained in the present numerical approach (where K_L/u^* can be obtained by writing $K_L/u^* = c^*/\Delta C$). Nevertheless, before discussing this comparison some comments about the values of K_L/u^* given by the computations are in order. First of all, comparison of the results obtained for $Sc = 1$ and for $Sc = 200$ confirms that the LES values follow a dependency close to Sc^m with $m = -0.5$. Actually, the slope of the line joining the results at $Sc = 1$ and $Sc = 200$ (Fig. 11) indicates a value $m = -0.516$ in the shear-free case and $m = -0.465$ in the sheared case. These results are close to the theoretical law but some deviation can be noticed. The reason for this departure comes from the fact that the theoretical law $m = -0.5$ is no more valid when the Schmidt number becomes of order unity. This was already pointed out in the case of a solid wall (where the theory predicts $m = -2/3$) by Kader and Yaglom (1972) and the LES results of Calmet and Magnaudet (1997) confirmed this trend. Moreover, recent computations were performed for the shear-free case at various Schmidt numbers ranging between 1 and 200 (Magnaudet and Calmet, submitted). These computations reveal that the $Sc^{-1/2}$ dependency is very well followed when the Schmidt number is O(100) while the exponent increases slightly for $Sc < 10$. For that reason, only the case $Sc = 200$ will be compared to the predictive models in the remaining of this section. In the sheared case, many experimental results are available for high Schmidt numbers. Hanratty (1991) compiled a lot of these results and concluded that the mass transfer coefficient follows the law $K_L/u^* = \alpha\ Sc^{-1/2}$ with α ranging between 0.12 and 0.15. The present result reported in Table 1 indicates $\alpha = 0.131$, showing that the predictions of the present LES approach are in very good agreement with the experiments.

To compare the present numerical predictions with available models it is necessary to determine the turbulent Reynolds number Re_T, the r.m.s. value of β and the bursting frequency. The integral scale required to estimate Re_T is obtained by

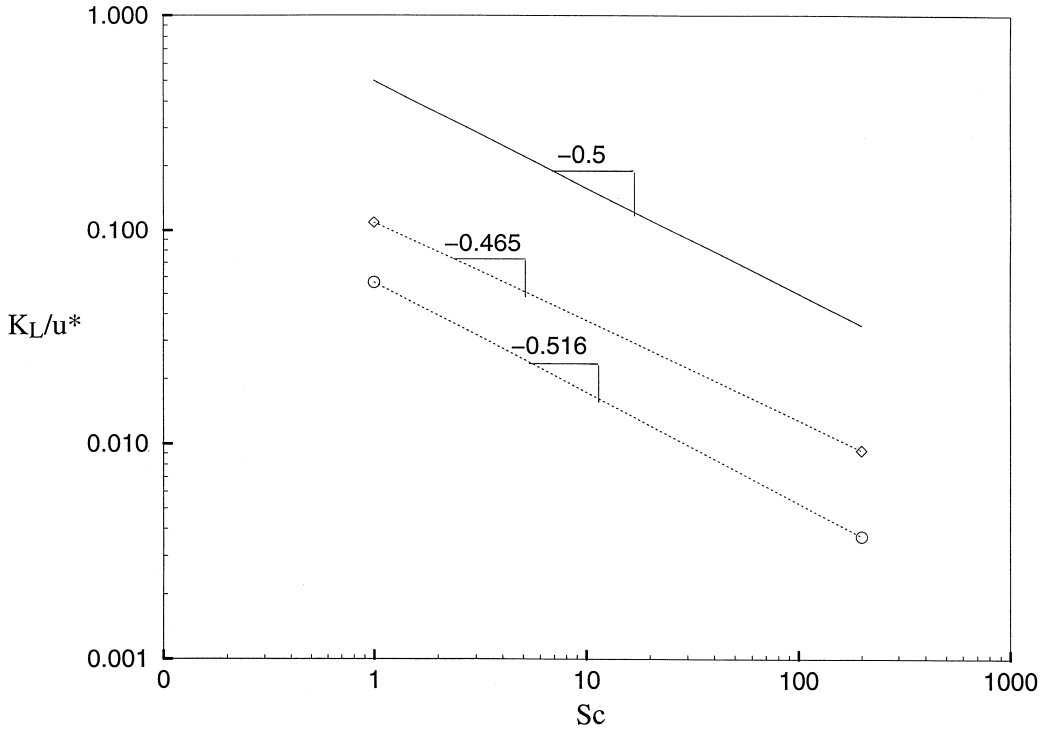

Fig. 11. Mass transfer coefficients K_L/u^*: ○ shear-free interface; ◇ sheared interface.

defining the scale ℓ related to the dissipation rate ε through $\varepsilon = u'^3/\ell$ and using the isotropic relation $L_\infty = \ell/2$. The value of $\langle\beta^2\rangle^{1/2}$ follows directly from the asymptotic behavior of the normal velocity fluctuation since it is given by the slope of $\langle v'^2\rangle^{1/2}$ in the viscous sublayer. Finally the bursting time can be estimated by determining the average distance between the bursts present at the surface and dividing by the mean streamwise velocity at the interface.

The key difficulty with the 'global' models lies in the location where Re_T is determined. Basically these models assume that the turbulence is homogeneous and isotropic while this is obviously not the case in the interfacial region. For example if one determines Re_T at a distance L_∞ from the interface (where the assumption of homogeneity is better verified), one finds $Re_T = 440$ for the sheared interface and $Re_T = 326$ for the shear-free case. Inserting these values in models (7) and (8) yields $5.1 \times 10^{-3} \leqslant K_L/u^* \leqslant 5.5 \times 10^{-3}$ and $2.91 \times 10^{-3} \leqslant K_L/u^* \leqslant 2.93 \times 10^{-3}$, respectively. It is obvious that these results underpredict significantly those found in the simulations. In contrast if one estimate the typical magnitude of the velocity fluctuation right at the interface, much higher values of Re_T emerge. Using these values one obtains the estimates of K_L/u^* reported in Table 1. These values are in much better agreement with those given by the simulations. One can remark that both models give fairly close predictions. This means that it is not possible to discriminate between the 'large scales' and 'small scales' models from the present simulations. Actually the two exponents of Re_T which appear in these models are rather close and the predictions become significantly different only for higher Reynolds numbers (Brumley and Jirka, 1988).

When the model (9) is applied to the sheared interface, Table 1 shows that the result is in very good agreement with the simulations. This confirms that the bursting events play a central role in the transfer. The problem is more complicated in the shear-free case. In that situation, a direct application of Eq. (9) leads to $K_L/u^* = 8.8 \times 10^{-3}$. This value clearly overestimates the result given by the LES. Banerjee (1990) observed a similar disagreement when he tried to apply his model to shear-free experiments. He argued that in that case only one part of the interface is covered by the large-scale structures which are active in the transfer, the remaining part being nearly inactive. This is clearly the case here as shown by Fig. 6. Banerjee overcame the problem by multiplying the value predicted by Eq. (9) by the percentage of 'active' surface. In the present case this percentage lies between 40% and 50%. The result of the 'corrected' model reported in Table 1 is then in good agreement with the simulations. Nevertheless the problem encountered in the application of model (9) to a shear-free interface underlines the intrinsic difficulty of the description of such interfacial conditions. Basically, this kind of turbulence is not produced in the vicinity of the interface, in contrast with the case where a strong interfacial shear is present. Thus the characteristics of this interfacial turbulence depends not only on the turbulence source itself (here the bottom wall) but also on the 'life' (and possibly 'death') of the turbulence during its

Table 1
Mass transfer coefficient predictions

	LES predictions	Large eddies (7)	Small eddies (8)	Bursting frequency (9)	Surface divergence (10)
Shear-free	3.70×10^{-3}	3.10×10^{-3}	3.40×10^{-3}	$(3.50–4.40) \times 10^{-3}$	4.36×10^{-3}
Sheared	9.29×10^{-3}	8.50×10^{-3}	1.17×10^{-2}	1.00×10^{-2}	1.00×10^{-2}

transport towards the interface. This means that at least an additional parameter, like the ratio between the integral scale and the distance between the region where the turbulence is produced and the interface, is needed to describe this situation.

Finally when the model (10) is applied, the results obtained in both flow configurations are found to be in very good agreement with the simulations even if a lower constant (0.6 instead of 0.71) would work better in the shear-free case. Keeping in mind that this model is based on the r.m.s. value of β which is nothing else that the divergence of the interfacial motions, this agreement found in two contrasted situations shows that β is indeed the key local parameter that governs the mass transfer rate. In other words, if one knows the rate at which the interface is dilated and compressed by the horizontal turbulent motions, the mass transfer efficiency can be readily predicted.

6. Conclusions

Large Eddy Simulation has been used to investigate high-Schmidt number mass transfer at a flat gas–liquid interface in the presence or in the absence of interfacial shear. Comparing the mass transfer coefficients found in the computations with the theoretical predictions has shown that the influence of the Schmidt number is correctly captured in the present approach. Statistics of the fluctuating concentration field have revealed the influence of both the Schmidt number and the local state of the turbulence. The mechanisms governing the mass transfer process have been clarified by examining the spatial structure of v' and c' close to both interfaces. Especially, it has been made clear that the turbulent events impacting the interface are the source of the concentration fluctuations. A comparison of the mass transfer coefficients given by the present approach with those predicted by simple available models has been carried out. The difficulties encountered with some of these models have been underlined and the central role of the surface divergence which is directly related to the limit behavior of v' has been confirmed. An essential point displayed by the present paper is the very good agreement observed between the mass transfer rates predicted by the LES approach and those found in the experiments. This agreement seems to be a very important result for two reasons. First it means that high-Schmidt number mass transfer can be studied without knowing all the details of the flow, especially by means of LES, which is a very good new from the methodological point of view. Second it suggests that the mass transfer process at a gas-liquid interface is governed by the large-scale motions because otherwise LES would have been unable to provide accurate predictions of the mass transfer rate. Obviously this point must be confirmed further, especially by varying the flow Reynolds number and looking at the dependency of the mass transfer coefficient with respect to Re_T. Looking at future developments, the present work suggest that at least two important points require deeper investigations. First of all, in the case of a sheared interface, capillary ripples are generally present in the experiments, so that the interface is generally rough, at least at small scales. Several theories have been developed in the past to take into account the role of these waves in the mass transfer process (see especially Coantic, 1986). Thus the question that comes to mind is: how is it possible that LES predictions based on a flat interface agree quantitatively with experiments performed with rough interfaces? An answer suggested by Banerjee (1990) could be that the ripples be the consequence of the impact of turbulent structures on the interface rather than a primary ingredient of the transfer. Another suggestion could be that the motions induced by capillary ripples are, to a large extend, two-dimensional and irrotational. If one accepts this idea, it seems reasonable to think that the interactions between these motions and the three-dimensional, rotational, turbulent motions are weak. In other terms the motions associated to capillary ripples could be nearly inactive in the mass transfer process, even if their intensity is of the same order as the one of the turbulence. Nevertheless these views have to be confirmed in order to specify the validity of present results. The second important question concerns the shear-free case. In that situation the interface sees a turbulent field produced elsewhere. Various systems like microjets, oscillating grids, submerged boundary layers can be used to produce this turbulence and the characteristics of the velocity field are different in all of them. Thus one important feature is to determine the turbulent characteristics which are intrinsically required for predicting accurately the mass transfer rate. For example, in models like (7) and (8), turbulence is characterized entirely by its intensity and its integral length scale. Thus one can wonder whether an open channel and an oscillating grid producing a turbulent field having the same kinetic energy and the same integral scale near the interface would lead to the same mass transfer rate. Accurate experimental and numerical studies performed with various turbulence sources are needed to clarify this point and, eventually, to derive new mass transfer models.

References

Banerjee, S., 1990. Turbulence structure and transport mechanisms at interfaces. In: Proceedings of International Conference Heat Transfer, Jerusalem.

Banerjee, S., Scott, D., Rhodes, E., 1968. Mass transfer to falling wavy liquid films in turbulent flow. Ind. Eng. Chem. Fundamentals 7, 22–27.

Brumley, B.H., Jirka, G.M., 1988. Air-water transfer of slightly soluble gases turbulence, interfacial processes and conceptual models. PCM PhysicoChemical Hydrodynamics 10, 295–319.

Calmet, I., 1995. Analyse par simulation des grandes échelles des mouvements turbulents et du transfert de masse sous une interface plane. Ph.D. Thesis, Inst. Nat. Polytech. Toulouse, France.

Calmet, I., Magnaudet, J., 1997. Large eddy simulation of high-Schmidt number mass transfer in a turbulent channel flow. Phys. Fluids 9, 438–455.

Coantic, M., 1986. A model of gas transfer across air–water interfaces with capillary waves. J. Geophys. Res. 91, 3925–3943.

Dankwerts, P.V., 1951. Significance of liquid film coefficients in gas absorption. Ind. Eng. Chem. 43, 1460–1466.

Fortescue, G.E., Pearson, J.R.A., 1967. On gas absorption into a turbulent liquid. Chem. Eng. Sci. 22, 1163–1176.

Germano, M., 1992. Turbulence: the filtering approach. J. Fluid Mech. 238, 325–336.

Germano, M., Piomelli, U., Moin, P., Cabot, W., 1991. A dy namic subgrid-scale eddy viscosity model. Phys. Fluids A 3, 1760–1765.

Hanratty, T.J., 1991. Effect of gas flow on physical absorption. In: Wilhelms, Gulliver (Eds.), Air–Water Gas Transfer. ASCE (Civil Engineers), New York.

Kader, B.A., Yaglom, A.M., 1972. Heat and mass transfer laws for fully turbulent wall flows. Int. J. Heat Mass Transfer 15, 2329–2351.

Lamont, J.C., Scott, D.S., 1970. An eddy cell model of mass transfer into the surface of a turbulent liquid. AIChE J. 16, 513–519.

Magnaudet, J., Calmet, I. Turbulence structure and mass transfer at a flat, shear-free, gas–liquid interface, submitted.

McCready, M.J., Vassiliadou, E., Hanratty, T.J., 1986. Computer simulation of turbulent mass transfer at a mobile interface. AIChE J. 32, 1108–1115.

Hunt, J.C.R., 1984. Turbulence structure and turbulent diffusion near gas–liquid interfaces. In: Brutsaert, Jirka (Eds.), Gas Transfer at Water Surfaces, pp. 67–82.

McLeish, W., Putland, G.E., 1975. Measurements of wind-driven flow profiles in the top millimeter of water. J. Phys. Ocean. 5, 516–518.

Zang, Y., Street, R.L., Kosseff, J.R., 1993. A dynamic mixed subgrid scale model and its application to turbulent recirculating flows. Phys. Fluids A 5, 3186–3196.